Evaluation method of ordinary flatbed scanners for quantitative density analysis

Satoshi Nishizuka[1,2], Newell R. Washburn[3], and Peter J. Munson[4]

[1]National Cancer Institute, National Institutes of Health, Bethesda, [2]SAIC-Frederick, National Cancer Institute at Frederick, Frederick, MD, [3]Carnegie Mellon University, Pittsburgh, PA, and [4]Center for Information Technology, National Institutes of Health, Bethesda, MD, USA

BioTechniques 40:442-448 (April 2006)
doi 10.2144/000112144

High-throughput microarray analyses require digitized images in order to convert the signal intensity to numerical values. To acquire the images, laser scanners are usually used for fluorescent signal detection. However, such microarray scanners have a limited number of excitation wavelengths, take minutes to scan a slide, and are expensive. In standard transcriptional array configurations, most study designs use relatively few samples against many probes, so only a small number of scans are necessary to complete the digital image acquisition for an experimental set. However, other microarray-based procedures may be more impacted by the limitations of dedicated microarray scanners. For instance, scanning is a major rate-limiting step when using high-density reverse-phase protein lysate microarrays (RPA) (Reference 1 and Figure 1A), which we have previously described as a method to perform proteomic profiling of many protein species across many samples. Because RPA signal detection employs a specific primary antibody followed by the catalyzed signal amplification colorimetric detection system (CSA; DakoCytomation, Carpinteria, CA, USA), whose final product is the dark-colored stain diaminobenzodine (DAB), signals can be obtained using the reflective mode of an ordinary optical flatbed scanner. Hence, we have been using optical flatbed scanners because of their fast scanning, relatively compact file size, and wide availability. However, there are several issues to be considered when using these scanners for quantitative applications.

Ordinary optical flatbed scanners are generally designed for capturing photographs in digitized format. Specifications of each scanner model are often not clear enough for quantitative analyses based on the manufacturer's information. For the use in quantitative analyses, several scanning factors should be clarified. For instance, resolution, dynamic range, bit depth, light source, and the software driver's characteristics can be important factors as any of them could influence the downstream analyses. It must be noted that digital data acquired from images are the product of all processes listed above, which are also characteristic of each scanner.

Since a scanner's specification information may be limited or unavailable, a calibrated material may be useful in estimating its performance (2,3). To examine dynamic range, bit depth, and most importantly, linearity in response to protein concentration, we used a wedge density strip (WDS; Danes-Picta, Praha, Czech Republic) including 20 calibrated reflective surfaces in each of 6 × 10 mm area, which can be mounted on a glass slide (Figure 1B). Raw pixel values of scanned images are converted into numerical values using the P-SCAN program (abs.cit.nih.gov/pscan) (1,4). Theoretically, the range of numerical values should be from 0 to 255 or 0 to 65,535 for 8- and 16-bit grayscale, respectively.

The WDS and RPAs were scanned with two ordinary flatbed scanners (Perfection 1250 and Perfection 4870; both from Epson, Long Beach, CA, USA). The scanning parameters were set as black and white photo, 600 dpi, and 8- and 16-bit grayscale for the Perfection 1250 and 4870, respectively. Numerical values corresponding to each sector of the density wedge strip were obtained using P-SCAN and were plotted against the optical densities measured by the manufacturer (Figure 2, A and B). Both the Perfection 1250 and 4870 demonstrated that they were able to utilize almost the full range of

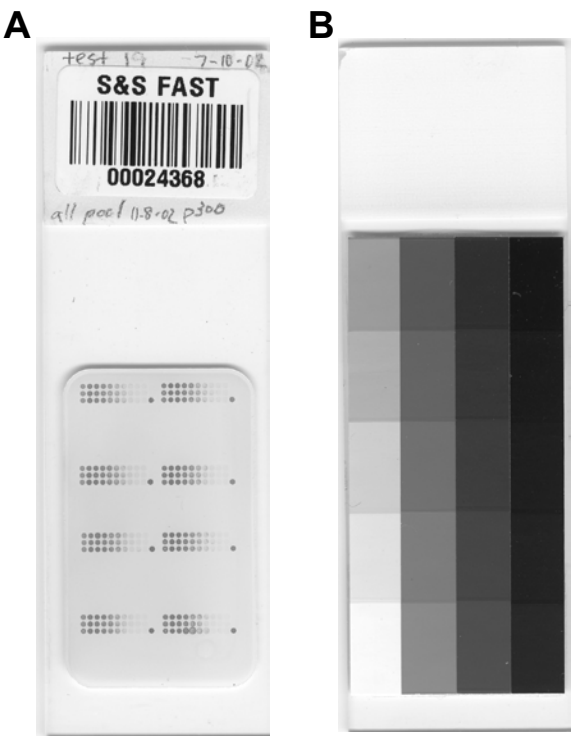

Figure 1. Reverse-phase protein lysate microarray (RPA) and wedge density strip (WDS). (A) RPA. Protein lysates from various cancer cell lines were mixed and spotted by a microarrayer (GMS417; Genetic MicroSystems/Affymetrix, Boston, MA, USA) onto glass slides embedded with nitrocellulose membranes. Each spot is approximately 600 µm in diameter. Each row represents one sample with 10 steps of a 2-fold dilution series. Therefore, theoretical protein concentration is log (base 2) scale from left to right. There are 24 rows on this array, all of which are the replicas. (B) The WDS mounted on a glass slide. There are 20 different sectors that differ in darkness from black to white. The optical density for each step in the scale was measured by reflective optical densitometry with a visual filter by the manufacturer.

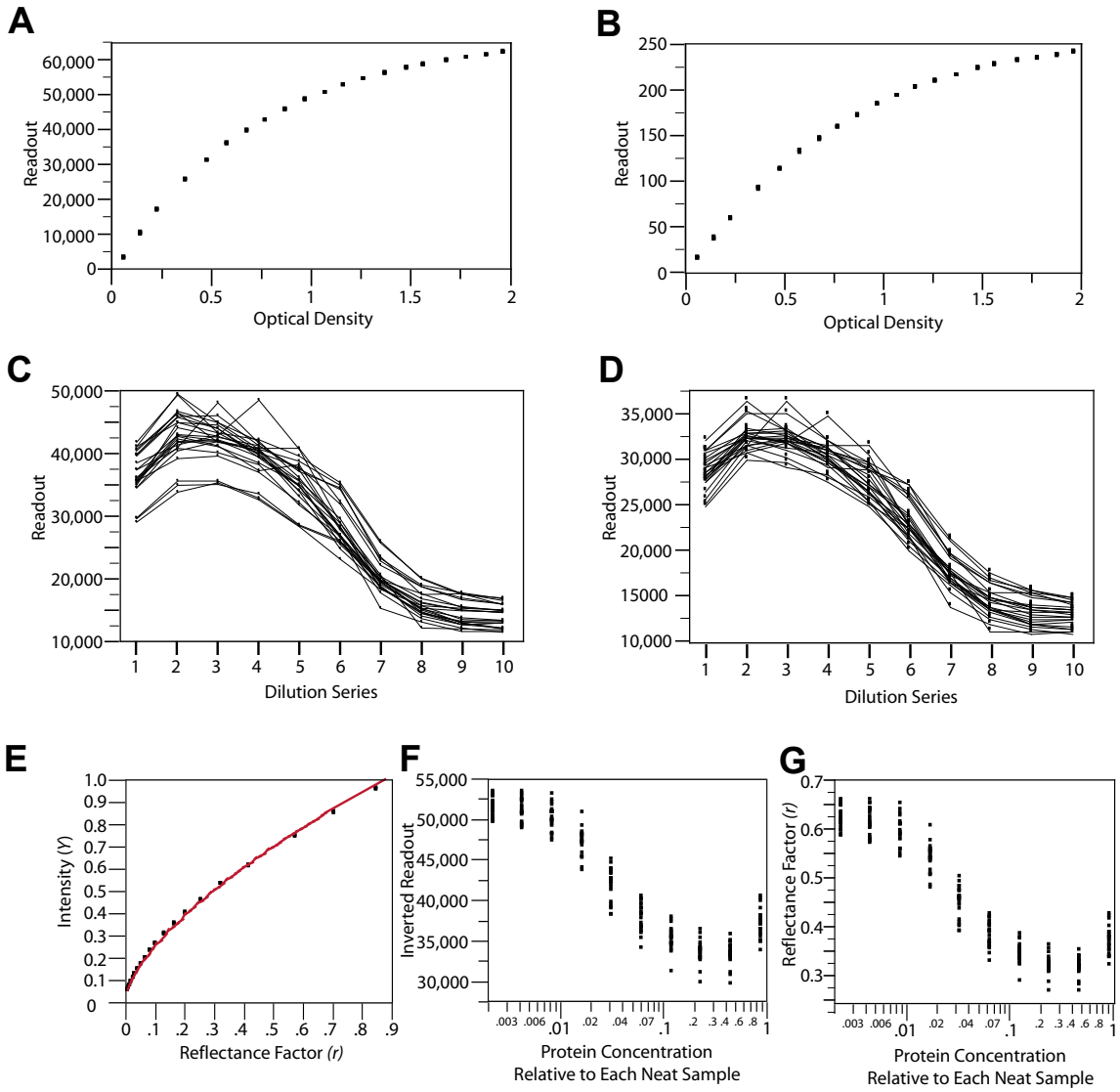

Figure 2. P-SCAN readout from the wedge density strip (WDS). (A) From a 16-bit scanner (Perfection 4870) and (B) an 8-bit scanner (Perfection 1250). Each step was measured at four different scanning points. The association between calibrated densities from the WDS and P-SCAN readout was logarithmic. (C) P-SCAN readout of reverse-phase protein lysate microarray (RPA) with the WDS, and without the WDS (D). Since this RPA has 24 replicated sets of 10-step serial 2-fold dilutions, each step of the dilution series has 24 data points. The x-axis indicates how many 2-fold dilutions have been performed. (E) A calibration curve for the normalized, inverted P-SCAN readout and reflectance factor *r*. (F) Relationship between theoretical protein concentration on the RPA slide and spot intensities from P-SCAN. The y-axis is inverted by being subtracted from 65,536. (G) Relationship between theoretical protein concentration on the RPA slide and the calibrated spot intensities expressed by *r*.

256 and 65,536 levels of grayscale. As expected, the plots level off at high optical density as a consequence of the theoretical limitation of the absorbance detection principle. Sequential mechanical adjustments (scanner hardware, scanning software, and graphical applications) may also limit the linear range. As a result, density-readout association could be slightly skewed or compressed.

Next, we scanned an RPA slide containing 24 replicated dilution series of a pooled set of lysates from 60 different cancer cell lines (1) (Figure 1A) that had been probed with an anti-p300 antibody and developed using the DAB chromogen system. Each of the 24 rows consists of a replicate set of 10 2-fold dilutions. We scanned the RPA with and without the WDS to see if the strip affects numerical values from the RPA. When the RPA was scanned by itself, the dynamic range within the RPA image was greater than when the test array was scanned with the density wedge strip (Figure 2, C and D). The darkest spot in the test array was nearly 50,000 in intensity value when it was scanned by itself, while the same spot showed a 35,000 intensity value when it was scanned with the WDS. This suggests that the scanner adjusts its gain automatically so that the scanner's sensor can recognize the lightest and darkest levels in the material. It may also suggest that intensity values may be controlled by the scanner's range determination algorithms and not based on the true intensity when a material is scanned by itself. Therefore intensity values that generated without the WDS

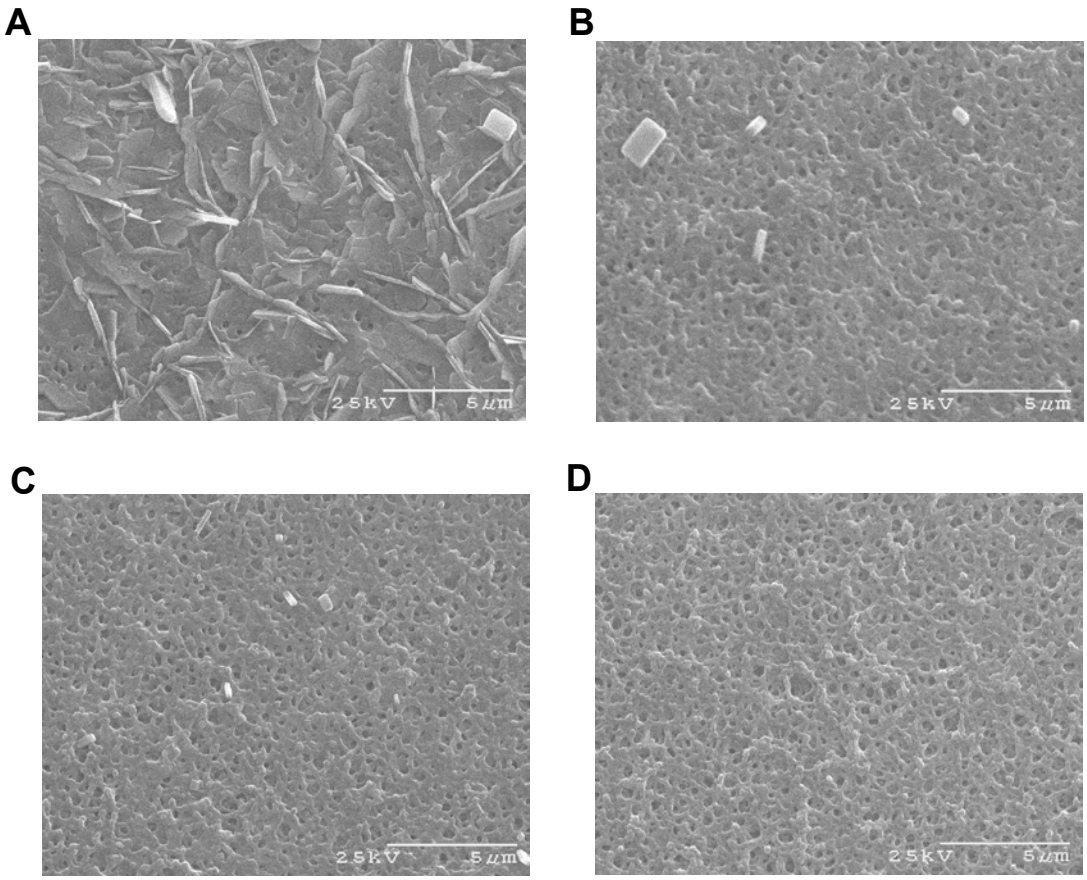

Figure 3. Electron microscopic images of spotted proteins on nitrocellulose membrane from a reverse-phase protein lysate microarray (RPA). Spotted protein lysates from the mixture of 60 different cancer cell lines were excised and subjected to scanning electron microscope (SEM). Specimens were attached to SEM stubs using double-stick tape or rubber cement and coated with gold using a SC-6 sputter coater (Pelco International, Redding, CA, USA). Specimens were examined using a Model 2460N scanning electron microscope (Hitachi, Tokyo, Japan). Digital images were obtained using the PCI Image management system software (Quartz Imaging Corporation, Vancouver, BC, Canada). (A) The highest concentration; proteins fill up the nitrocellulose pore structure. (B) Second highest concentration; the pore structure is becoming visible. (C) Third highest concentration; more pore structure is visible. (D) The lowest concentration; it is close to the nitrocellulose without protein. More pores and three-dimensionally expanding pores are visible. Scale bar, 5 μm.

may represent artifactual levels that are unique to the scanner.

It should be noted that in Figure 2, C and D, there is a zero derivative in the dose-response curve that corresponds to the samples near the highest protein concentrations. This phenomenon has been seen often, and we speculate that this may be due to an excess of nontarget antigens that hide the target antigen. Moreover, electron microscopic examination of the spotted protein on the nitrocellulose revealed that highest concentration spots have fewer pores on the surface, which may prevent antibodies from accessing antigens in the liquid phase as they migrate under capillary attraction (Figure 3).

At lower protein concentration levels, the signal levels off to a minimum corresponding to a readout value of about 10,000–15,000. We believe that this high level of background is due to the properties of the nitrocellulose that coats the glass slides. In other words, nitrocellulose appears to be substantially darker than pure white. In previous studies, we have shown that negative control slides incubated with a mouse monoclonal antibody whose antigen does not exist in humans (*Aspergillus niger* glucose oxidase), but whose structure is the same as other monoclonal antibodies, does not contribute significantly to background (1).

Next, we attempted to improve the assay linearity by using the WDS readings to calibrate the RPA data. To generate a calibration curve, the scanner readouts corresponding to the WDS scan were first inverted (subtracted from 2^8 or 2^{16}, so that zero readout represented black) and scaled (so that 1 represented white). Then the manufacturer-provided optical densities for each sector of the wedge strip were converted to reflectance factor values, *r*. In brief, the WDS density values are described as reflective optical densities (*D*) according to ISO 5 (International Standards Organization 5) geometry of input/output flux = 45/0 degrees relative to the surface normal (5), measured by visual filter. Optical density *D* is the negative common (base 10) logarithm of the reflectance factor *r*. The reflectance factor is the proportion of the luminous flux reflected by a sample, Φ, to that reflected by the perfect reflected diffuser, Φo. Therefore, *r* can be expressed:

$$r = \Phi/\Phi o$$

and,

$$D = -\log r$$

A plot of intensity (inverted, scaled readout) versus r is shown in Figure 2E. A curve was fit to these data points, and the following equation was determined:

$$Y = 1.091321121 \times r^{0.6415541}$$

where Y is the normalized, inverted readout and r is the reflectance factor. Figure 2F shows a plot of inverted readout (unscaled intensity) as a function of protein concentration; this graph represents uncalibrated data. In Figure 2G, calibrated data are shown. Experimental intensity values were plugged into the preceding equation, and r values were calculated. Despite this process, there was no visible difference between raw and calibrated data (Figure 2, F and G). We speculate that the limited range of RPA densities made the effect of calibration minor.

The use of the WDS revealed that ordinary scanners have the capacity to utilize nearly the full theoretical dynamic range, to reasonably distinguish small step densities, and that linearity is not affected by calibration due to the small range of intensities on RPA. Although the WDS-based calibration had little practical effect, the use of a WDS would be useful to determine where the experimental intensities are located in terms of density. This constant density scale should be a good standard across different experiments or scan runs, or scanners, which should facilitate quantitative data analysis in a more sophisticated manner. Finally, by addressing the quality issues of ordinary flatbed scanners for quantitative analysis, we have shown ordinary flatbed scanners have application for array-based techniques such as RPA, in which scanning speed is a major rate-limiting process.

ACKNOWLEDGMENTS

We thank Mr. Joseph Suhan for help with scanning electron microscope. The content of this publication does not necessarily reflect the views or policies of the Department of Health and Human Services, nor does mention of trade names, commercial products, or organization imply endorsement by the U.S. Government. This project has been funded in whole or in part with Federal funds from the National Cancer Institute, National Institutes of Health (NIH), under contract no. NO1-CO-12400, and from the Center for Information Technology, NIH.

COMPETING INTERESTS STATEMENT

The authors declare no competing interests.

REFERENCES

1. **Nishizuka, S., L. Charboneau, L. Young, S. Major, W.C. Reinhold, M. Waltham, H. Kouros-Mehr, K.J. Bussey, et al.** 2003. Proteomic profiling of the NCI-60 cancer cell lines using new high-density reverse-phase lysate microarrays. Proc. Natl. Acad. Sci. USA *100*:14229-14234.
2. **Alva, H., H. Mercado-Uribe, M. Rodriguez-Villafuerte, and M.E. Brandan.** 2002. The use of a reflective scanner to study radiochromic film response. Phys. Med. Biol. *47*: 2925-2933.
3. **Thomas, G., R.Y. Chu, and F. Rabe.** 2003. A study of GafChromic XR Type R film response with reflective-type densitometers and economical flatbed scanners. J. Appl. Clin. Med. Physiol. *4*:307-314.
4. **Carlisle, A.J., V.V. Prabhu, A. Elkahloun, J. Hudson, J.M. Trent, W.M. Linehan, E.D. Williams, M.R. Emmert-Buck, et al.** 2000. Development of a prostate cDNA microarray and statistical gene expression analysis package. Mol. Carcinog. *28*:12-22.
5. **Proctor, J.E. and P.Y. Barnes.** 1996. NIST high accuracy reference reflectometer-spectrophotometer. J. Res. Natl. Inst. Stand. Technol. *101*:619-627.

Received 24 August 2005; accepted 18 January 2006.

Address correspondence to Satoshi Nishizuka, Molecular Translational Technologies, Molecular Therapeutics Program, National Cancer Institute, National Institutes of Health, Building 37, Room 1126-B, 9000 Rockville Pike, Bethesda, MD 20892, USA. e-mail: nishizus@mail.nih.gov